

Short Communication

Effect of pH Values on the Characterization of Electrodeposited Zn–Mn Coatings in Chloride-Based Acidic Environment

Metin Bedir^{1,*}, Derya Korkmaz¹, Omer F. Bakkaloglu¹, Mustafa Oztas², İsmail H. Karahan³ and M. Yakup Hacıbrahimoglu⁴

¹University of Gaziantep, Engineering Physics Department, Gaziantep/TURKEY

²University of Yalova, Chemistry and Process Engineering, Yalova/TURKEY

³University of Musfata Kemal, Physics Department, Antakya/TURKEY

⁴University of Gaziantep, Department of Metallurgical and Materials Engineering, Gaziantep/TURKEY

*E-mail: bedir@gantep.edu.tr

Received: 24 January 2015 / Accepted: 5 April 2015 / Published: 28 April 2015

Effect of processing pH on structure and corrosion resistance of Zn-Mn coatings deposited on AISI 4140 high tensile steel in chlorine based sulphate baths by potentiostatic technique at a constant potential of -2 V was investigated. Structural analyses on the coatings were performed by X-ray diffraction (XRD), scanning electron microscopy (SEM), and energy-dispersive X-ray spectroscopy (EDX). Cyclic voltammetry (CV) and linearly sweep voltammetry (LSV) were used to determine the potential ranges of coated surface where the various redox processes take place. The general corrosion rate of coatings were calculated by using the corrosion parameters such as linear polarization resistance (LPR), corrosion current (I_{corr}) and Tafel slopes (b_c and b_a)

Keywords: Electrodeposition, XRD, Corrosion. PACS: 82.45.Qr; 61.10.Nz; 82.45.Bb.

1. INTRODUCTION

Development of corrosion resistant structural components is an essential task in engineering activities. Corrosion is an important factor regarding damage and failure of metallic materials. Surface of an alloy plays an important role in growth of highly adhering mechanically intact films and their corrosion performance and degree of corrosion resistance of surfaces are important factor for their use in different applications. Zinc and its alloys are extensively used for high resistive protection of ferrous type materials in industry recently. Several authors have reported on the corrosion behavior of Zn and its alloys, particularly Zn-Fe, Zn-Co and Zn-Ni, in some corrosive environments. As a result of these

reports, Zn-Mn alloys have even better corrosion resistance [1,2]. Zn-Mn layers can be electrodeposited using simple sulphate baths [2] containing citrates [3, 4], chloride baths [5], fluorborate baths [6], and acidic baths containing EDTA [7]. Several authors have reported that Zn-Mn alloy coatings can supply a reasonably well corrosion resistance in aggressive environments that contains sodium chloride and sulphur dioxide [8–10]. Zn-Mn characterize with higher corrosion resistance and also higher ability against the substrate than pure zinc. Performance of Zn-Mn alloy coatings on steel against general corrosion was superior to that of the coatings of each individual metal. The Zn-Mn alloy is a metallic sacrificial anode material that has not been widely studied, especially for coating applications. This alloy is mainly used for aeronautical and marine applications. Its corrosion resistance in atmospheric and chloride containing sea water environments is valuable for those applications. However, the protection is not appreciable under severe atmospheric conditions and with alternative substrates of materials. Among those materials are the Zn-Mn alloys, which seem to display both improved corrosion resistance and environmental compatibility. A variant (or an alternative) to the alkaline bath, for Zn-Mn alloy deposition, was reported by several authors [11–15], which revealed even better corrosion protective coating. It has been reported that alloy coatings with a high Mn content (10-30 at. % Mn) show the highest corrosion resistance known among zinc alloys [16, 17]. The objective of the present paper was to study the influence of pH values of electrolytes in electrochemical deposition process of Zn-Mn alloys on AISI 4140 stainless steel. The corrosion behaviour of Zn-Mn alloys obtained in pyrophosphate solution revealed correlations relevant with phase composition, morphology of deposited coatings, and corrosion resistance of the coatings.

Electrodeposition technique with three-electrode system is easy, cheap, suitable to the other depositions which are organic or phosphating or another coating techniques. The uses of these methods have been forbidden due to adverse effects on human health and the environment in recent years.

Electrodeposition of metallic layers is mostly used to modify the substrate surface for producing a broad range of useful materials with improved mechanical, electrochemical, electrical, magnetic or optical properties. Thus, less expensive materials can be used as substrates, making this process economically attractive. Compared to pure metal coatings, alloy coatings obtained by electrodeposition show better properties, since their chemical composition can be varied to the required function. Moreover, because of involving control of several chemical and operational parameters, alloy electrodeposition is rather complex than single metal deposition. The parameters of the alloy electrodeposition are often chosen empirically, in practice. Therefore, it is important to develop a more scientific approach leading to a better fundamental understanding of codeposition phenomenon. This will lead to improved processing performance and reliability, as well as establishing of new alloy systems [18].

2. EXPERIMENTAL DETAILS

All test solutions were made using analytical grade chemicals (Sigma Aldrich) and doubly distilled (DD) water. The electrochemical experiments were carried out in a three electrode glass cell receiving disc shaped specimens made out of 12 mm diameter and 1mm thick AISI 4140 stainless steel

of working electrode, a platinum mesh counter electrode (surface area), and a commercial saturated calomel (SCE) reference electrode (that is 224 mV nobler to standard hydrogen electrode). The working electrode was an AISI 4140 stainless steel having typical composition of ; %0.36 C, %0.80 Mn, %0.005 Si, %0.914 Cr, %0.30 Ni, %0.85 Mo, %0.075 V, %0.07 S, %0.143Cu ve %0.034 P with an effective surface area of 0.78 cm^2 . All potentials are reported with respect to this reference. Prior to the experiments, the steel discs were polished with silicon carbide emery paper, sonicated for 5 min, and rinsed thoroughly with Millipore Milli-Q ultrapure water. Electrodeposition of Zn–Mn alloys was performed galvanostatically, at current densities of $10\text{--}90 \text{ mA/cm}^2$. Deposition times were managed to obtain layers of $10 \mu\text{m}$ in thickness. The composition of the electrolyte was as follows: 0.1 mol/L ZnCl_2 , 0.1 mol/L $\text{MnCl}_2 \cdot 4\text{H}_2\text{O}$, 2.8 mol/L KCl, 0.3 mol/L H_3BO_3 without additives similar in previous study (Trejo et al., 2008) [19] and tested results show a good corrosion properties including various pH values in the 3-6 range. The pH value of the solution was adjusted by adding hydrochloric acid and NaOH in the range of 3-6. Cyclic voltammetry was used to determine potential ranges of various redox processes taking place over the coated surface. The experiments were performed at room temperature with a CHI100 potentiostat system, a product of CH Instruments, Inc. (3700 Tennesion Hill Drive 1, Austin, TX 78738 1, USA). Prior to the potential scans the steel electrodes were left at the open circuit potential for 10 s. The composition, structure, and the morphology of deposits were studied by scanning electron microscopy (SEM), energy dispersive X-ray spectrometry (EDS), and X-ray diffraction (XRD).

The potentiodynamic measurements were done in the same electrochemical cell containing aqueous solution of 3.0 wt. % NaCl at pH 7.0. Samples with active surface areas of 1 cm^2 were mechanically polished with diamond paste to a roughness of $3 \mu\text{m}$, then thoroughly rinsed with distilled water, and placed in the measurement cell immediately as wet. When a stable corrosion potential E_{corr} was reached approximately in 30 minutes, potentiodynamic polarization tests were run with an automatic potential shift at a scanning rate of 10^{-3} V/s . Polarization for each sample was started at a potential of -1500 mV vs SCE shifting towards the anodic side till a clear increase in the current density was observed. The quantitative composition analysis of the electrodeposits was carried out by JEOL 6400 scanning electron microscope (SEM) with energy dispersive spectrometer (EDS) working at 15-30 kV. Preferrantial crystal orientations of the deposits on the steel surface were determined by X-ray diffraction (XRD) analysis, using a Philips PANalytical X'Pert Pro X-ray diffractometer with $\text{CuK}\text{-}\alpha$ radiation (1.5418 \AA). The 2θ diffraction angle range of $10^\circ\text{--}90^\circ$ was recorded at a rate of $0.02^\circ/2\theta/0.5 \text{ s}$. The crystal phases were identified comparing the acquired 2θ values and their intensities.

3. RESULTS AND DISCUSSION

The influence of pH on deposition of Zn-Mn alloy was studied using cyclic voltammetric method. Fig.1 shows the typical voltammograms obtained from the optimized bath solutions in presence and with different pH values. The main information about components of the alloy and structure of the deposited phases is given by the voltammetric response.

The scans were initiated at near open circuit potentials. During the forward scan towards the negative direction, the cathodic current increased sharply when the deposition begins in solutions. In Fig.1, it can be observed from the cyclic voltammograms that the increase of the electrolyte pH, caused a decrease of the dissolution peak except for pH=6.

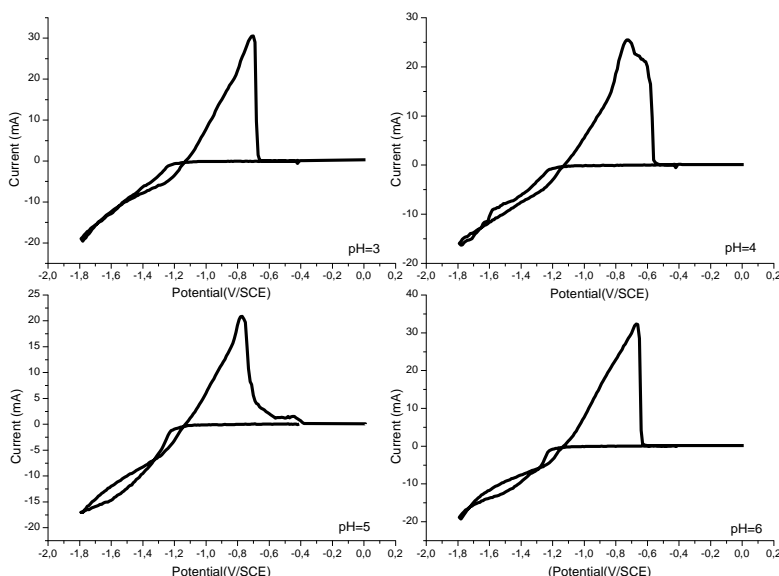


Figure 1. The typical cyclic voltammograms of Zn-Mn alloy deposited in solutions with different pH values.

This peak is in agreement with the preferential dissolution of zinc, so the decrease of dissolution peaks can be related to the composition of the dissolved deposit. It can be attributed that an increase in the bath pH causes a decrease in the rate of zinc deposition except pH=4, causing the observed decrease in size of dissolution peaks.

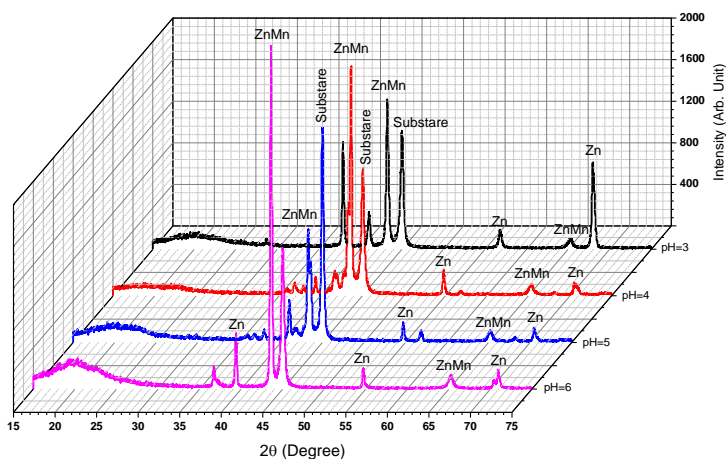


Figure 2. X-ray diffraction patterns of Zn–Mn alloy coatings with different pH values of processing electrolyte.

Fig.2 shows the XRD patterns of the samples obtained in the baths with different pH values. The preferential crystal orientation of the electrodeposits depends on the experimental conditions [20,21] such as pH, current density [22] and temperature [23]. The XRD pattern shows the formation of lines corresponding to of a mixture of Zn phase and hexagonal close packed ϵ -phase Zn–Mn phase with different crystallographic orientations [19]. The phases of the electrodeposited Zn–Mn alloy depend on the chemical compositions with various co-precipitation pH values. XRD peaks of all samples are broadened, but peak widths decrease with the increasing pH value, which indicates that the average crystalline size for the deposited layers gradually increases with increasing pH value until 6, except for the layer of pH value of 5. When pH value is 5, the peak intensities became weaker due to the dissolution of zinc hydroxide in the high pH solution.

Table 1. Relative amounts of the Zn and Mn in the films deposited with different pH values

| | % Zn | % Mn |
|------|-------|-------|
| pH 3 | 94,85 | 5,15 |
| pH 4 | 93,23 | 6,77 |
| pH 5 | 89,16 | 10,84 |
| pH 6 | 95,46 | 4,54 |

The EDX results showing the relative amounts of the Zn and Mn in the films deposited with different pH values are shown in Table 1 from which one can see the relative atomic percentage of Mn in the deposited films increases with increasing pH until pH value of 6. Further increase in pH affects Mn deposition negatively.

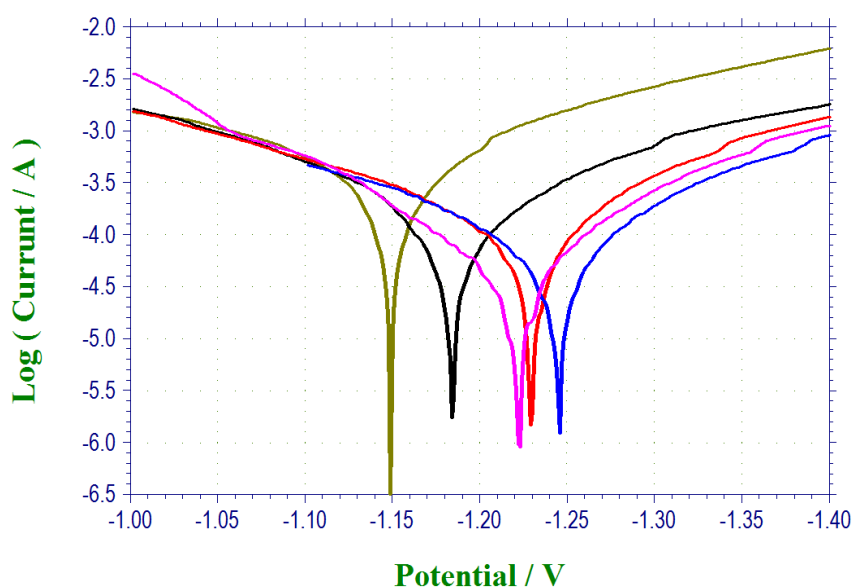


Figure 3. Potentiodynamic polarization behavior of electrodeposited Zn–Mn alloys on AISI 4140 substrates in 3% NaCl solution for different pH values. a) green: AISI 4140, b) black: pH=3, c) red: pH=4, d) blue: pH=5, e) pink: pH=6.

These results can be confirmed by XRD patterns shown in Figure 2. The bulged region seen at about 42-45 degree which can be attributed to partially crystalized (nearly amorphous) Mn-rich β_1 -phase [24] swells as pH increases. This supports the increase of Mn amount in the films. Intensity of the peak corresponding Zn-rich η -phase increased with increasing pH values. This increment in the peak corresponds to β_1 -phase has been accompanied by the increase in η -phase until pH value of 6. As can be seen, the bulged region vanished at pH 6 value. As a result of this relative amount of Mn firstly increased and then decreased sharply.

The potentiodynamic polarization curves, which were performed using steel that was coated galvanostatically by Zn–Mn alloys at different pH values, are shown in Figure 3 in which the variation of current density versus potential is indicated. For comparison, polarization curve of AISI 4140 steel is also shown with that of coated Zn-Mn alloys in this figure and the corrosion potentials of Zn-Mn alloys and AISI 4140 steel were ascertained. The corrosion current density (I_{corr}) and corrosion potential (E_{corr}) were obtained from the intercept of the Tafel slopes. The whole observations about corrosion current density (I_{corr}) and corrosion potential (E_{corr}) are listed in Table 2. It was observed that the increasing amount of the corrosion current (I_{corr}) with the increase in the pH values. Therefore, the measured corrosion potentials have values that are more negative, and the alloy exhibits better corrosion resistance at pH=5. As the pH increased in the range of 3–6, the peaks were shifted negatively. It is indicated that the smallest corrosion potential (E_{corr}) was measured as -1.184 V vs SCE for Zn-Mn alloys coated at pH=3 and the biggest one as -1.246 V vs SCE at pH=5. When the comparison of corrosion potentials take place, the coated alloy at pH=5 is 13% nobler than at pH=3. When the pH value of Zn-Mn solution increases as can be seen from figure that the corrosion potential shifts to the higher values at which it behaves nearly nobler indicating that the pH value can improve the stability of the passivation film and the corrosion resistance.

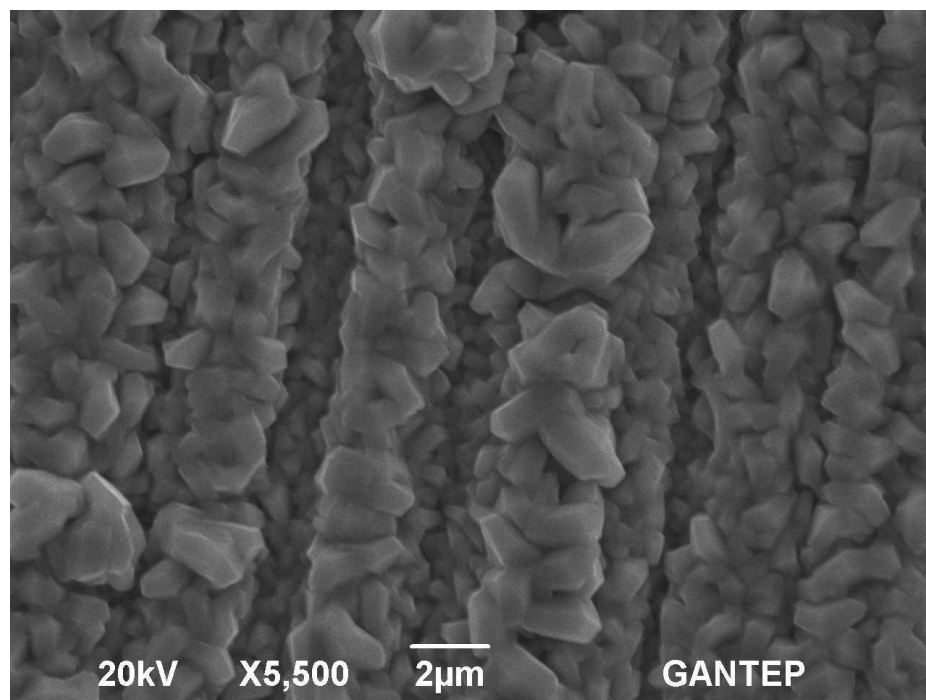
Table 2 the list of samples with variations in pH values, E_{corr} and I_{corr} respectively.

| Samples | pH values | E_{corr} (Volt) | I_{corr} (mA) |
|-----------------------------|-----------|--------------------------|------------------------|
| AISI 4140 Steel (Substrate) | - | -1,149 | -0,8851 |
| ZnMn | 3 | -1,184 | -0,4446 |
| ZnMn | 4 | -1,229 | -0,3047 |
| ZnMn | 5 | -1,246 | -0,3126 |
| ZnMn | 6 | -1,223 | -0,3033 |

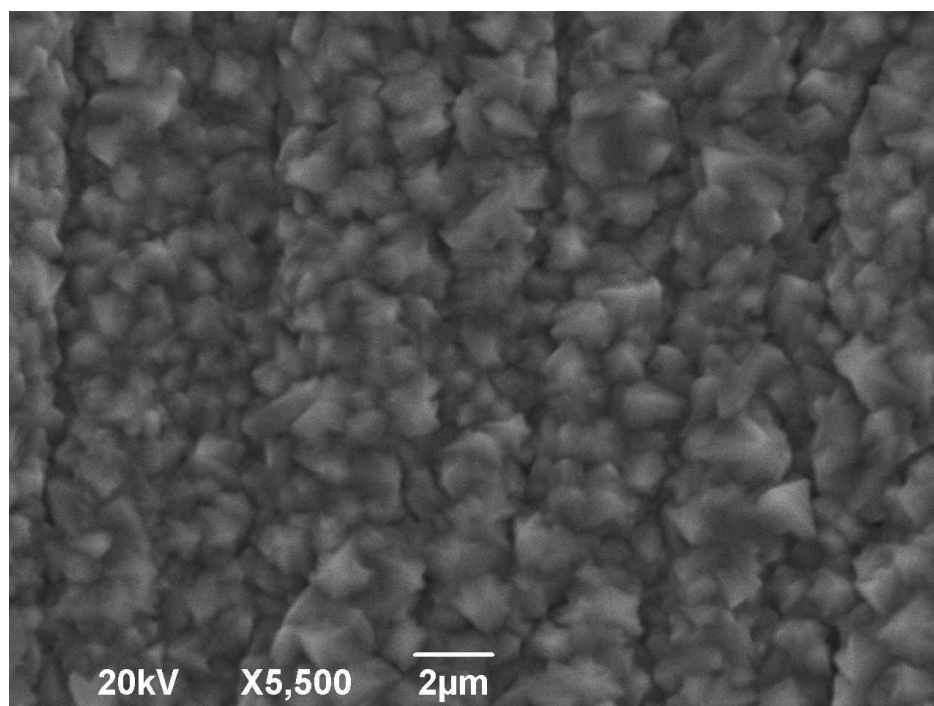
In general the best corrosion was obtained at pH=5. This higher corrosion resistance can attribute to a higher Mn content in the film. Mn favours and accelerates the formation of passive film on the surface of the substrate (AISI 4140 steel). This result supports the former studies [19].

All zinc alloys have also more positive corrosion potentials but a less negative than that of AISI 4140 steel substrate, which indicates that the Zn–Mn coating is an ideal cathodic protective coating for steel products. Zn-Mn coating can provide longer protection for steel products than pure zinc coatings due to the smaller free corrosion potential difference between the Zn-Mn coating and that of steelbase substrate. Generally, the active dissolution ability of materials is determined by using corrosion current density and corrosion potential [25], while passivation potential is used to determine the passivation

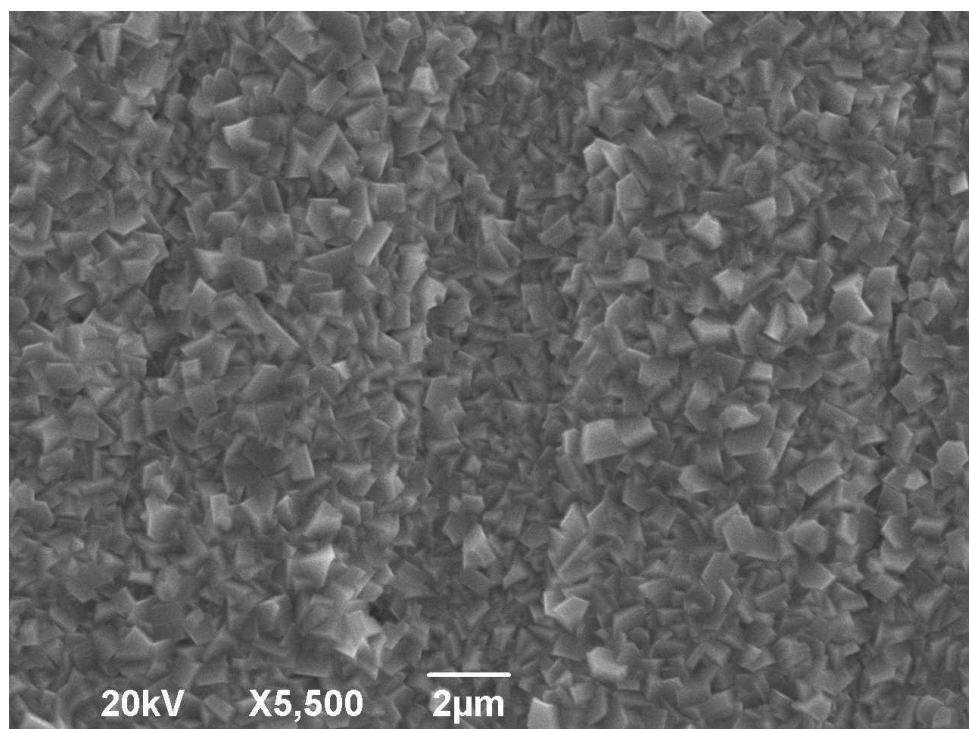
ability of materials, the chemical stability and corrosion resistance of passive films are evaluated by the aid of the passive current density and passive range [26].



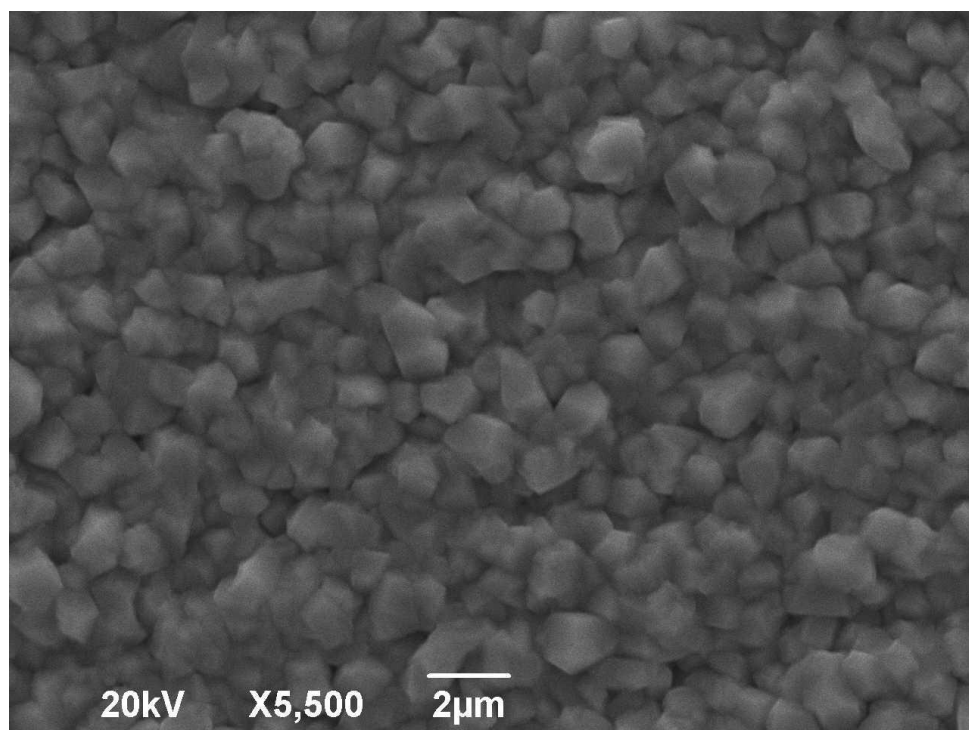
a) pH=3



b) pH=4



c) pH=5



d) pH=6

Figure 4. SEM images of the Zn-Mn coatings, a) pH=3, b) pH=4, c) pH=5 and d) pH=6.

Fig.4 shows the SEM images of the samples electrodeposited at different pH values of the electrolyte. It is observed that the deposits are generally composed of fine grains. This could be attributed to a large polarization that accompanies the deposition process. Large polarization promotes the nucleation rate over the growth rate [27]. As it can be seen from SEM figures, the average size of the coating particles decreases with increasing pH of the electrolyte up to pH=5. Then the average grain size increases with increasing pH value to 6. It is understood from these figures that bath pH plays the role of a grain-size refiner at Zn-Mn alloys, similar results have been seen by other researchers for electrodeposition of different alloys or composites, e.g. Zn-Ni-Fe [28] and Nickel-layered Silicate nanocomposites [29]. These results suggest that pH of the electrodeposition bath is closely associated with deposition properties such as average size of particles and density and compactness of resultant coating film. From the above mentioned results, it can be concluded that the best coating film in terms of uniformity and compactness is obtained from electrolyte bath pH=5. After the comparison of all Zn-Mn films on the substrate, the finer grained structure was observed at grown with pH=5 bath. This actually means that a better corrosion stability occurs because of the small grain size creating more grain boundaries that acts as a corrosion barrier [30]. The density of the grain boundaries increases which provides to increase of active sites with decreasing of grain size. This increment in active sites favors the expeditiously formation of sustained and protective film [31]. It is postulated that with increase in the pH value up to 5, when the value of overpotential rises, free energy for formation of new nuclei in Zn-Mn alloy deposits increases leading to higher nucleation rate and so that the formation of coatings with smaller grain size takes place. However, further increment in the pH value up to 6 causes in creation of discrete large crystallites. The formation of big and discrete polyhedral grains is referable to the fast growth of grains and accumulation on the nuclei in comparison with nucleation rate [32].

4. CONCLUSIONS

In this work we investigated various Zn-Mn alloy coatings deposited by typical three electrode system in brackish aqueous solutions at different pH values. The corresponding electroplating behavior and corrosion properties of Zn-Mn alloys were investigated using cyclic voltammetry method. The effect of bath pH was investigated on the structure of Zn-Mn alloys, and the corrosion behaviour of AISI 4140 steel substrates. The average size of the particles in coatings decreased with increase in pH of the processing electrolyte. The pH of the coating bath was closely correlated with structural, contextual and morphological, consequently with corrosion resistance properties of the coated films. The most corrosion protective coating produced in this work was the one, that was deposited at pH 5 corresponds to relatively higher Mn amount.

ACKNOWLEDGEMENTS

This study is supported from University of Gaziantep, Scientific Research Projects Unit (BAPYB) by a research project number of MF.09.07.

References

1. G. D. Wilcox, B. Petersen, *Trans. Inst. Met. Finish.* 74 (1996) 115.
2. N. Boshkov, *Surf. Coat. Technol.* 172 (2003) 217.
3. M. Eyraud, A. Garnier, F. Mazeron, J. Crousier, *Plat. Surf. Finish.* 82 (1995) 63.
4. D. R. Gabe, G.D. Wilcox, A. Jamani, *Metal Finishing* 91 (1993) 34.
5. D. Sylla, J. Creus, C. Savall, O. Roggy, M. Gadouleau, Ph. Refait, *Thin Solid Films* 424 (2003) 171.
6. Y. Sugimoto, T. Urakawa, M. Sagiya, Extd. Ads. 179th Electrochem. Soc. Meeting, Washington DC, USA, 5–10 May, 1991 91(1) 831.
7. C. Muller, M. Sarret, T. Andreu, *J. Electrochem. Soc.* 149 (2002) C600.
8. M. Eyraud, A. Garnier, F. Mazeron, J. Crousier, *Plat. Surf. Finish* 82 (1995) 63–70.
9. B. Bozzini, E. Griskonis, A. Fanigliulo, A. Sulcius, *Surf. Coat. Technol.* 154 (2002)294–303.
10. N. Boshkov, *Surf. Coat. Technol.* 172 (2003) 217–226.
11. M. Sagitama, T. Urakawa, T. Adaniya, T. Hara, *SAE Tech. Papers* 860 (1986) 268.
12. G. Govindarajan, V. Ramakrishnan, S. Ramamurthi, V. Subramanian, N.V.
13. Parthasaradhy, *Bull. Electrochem.* 5 (1989) 422.
14. D.R. Gabe, G.D. Wilcox, A. Jamani, B.P. Pearson, *Met. Finish.* 91 (1993) 34.
15. G.D. Wilcox, B. Petersen, *Trans. Inst. Met. Finish.* 74 (1996) 115.
16. J. Crousier, F. Soto, M. Eyraud, *Mater. Tech.* 3–4 (1999) 47.
17. C. Muller, M. Saret, T. Andreu, *J. Electrochem. Soc.* 149 (2002) C600
18. L. Diaz-Ballote, R. Ramanauskas, P. Bartolo-Perez, *Corros. Rev.* 18 (2000) 41.
19. L. F. Senna, S. L. Diaz, L. Sathler, *J. Applied Electrochem.* 33 (2003) 1155-1161.
20. P. Díaz-Arista, Z.I. Ortiz, H. Ruiz, R. Ortega, Y. Meas, G. Trejo, *Surface & Coatings Technology*, 203(2009) 1167-1175.
21. J. B. Bajat, V. B. Miskovic-Stankovic, M. D. Maksimovic, D. M. Drazic & S. Zec, *Electrochim Acta*, 47(2002) 4101-4112.
22. Y. Oren & U. Landau, *Electrochim Acta*, 27(1982) 739-748.
23. M. Bucko, J. Rogan, S.I. Stevanovic, A. Peric-Grujic, J.B. Bajat, *Corrosion Science* 53 (2011) 2861.
24. C.-H. Liang, C.-S. Hwang, *Journal of Alloys and Compounds* 500 (2010) 102.
25. M. Bucko, J. Rogan, B. Jokic, M. Mitric, U. Lacnjevac, J.B. Bajat, *Journal of Solid State Electrochemistry* 17 (2013) 1409.
26. P. Roberge, *Handbook of Corrosion Engineering*, McGraw-hill, 1999.
27. S.H. Tuna, N.Ö. Pekmez, F. Keyf, F. Canlı, *Dental Materials* 25 (2009) 1096.
28. L. Guo, P.C. Searson, *Electrochimica Acta* 55 (2010) 4086.
29. M. Abou-Krisha, *J Coat Technol Res* 9 (2012) 775.
30. J. Tientong, C.R. Thurber, N. Souza, A. Mohamed, T.D. Golden, *International Journal of Electrochemistry* 2013 (2013) 8.
31. L.-y. Qin, J.-s. Lian, Q. Jiang, *Transactions of Nonferrous Metals Society of China* 20 (2010) 82.
32. A. Balyanov, J. Kutnyakova, N.A. Amirkhanova, V.V. Stolyarov, R.Z. Valiev, X.Z. Liao, Y.H. Zhao, Y.B. Jiang, H.F. Xu, T.C. Lowe, Y.T. Zhu, *Scripta Materialia* 51 (2004) 225.
33. A. Milchev, *Electrocrystallization: Fundamentals of Nucleation and Growth*, Springer, 2002.